Eur. Phys. J. D **38**, 139–141 (2006)
DOI: 10.1140/epjd/e2005-00253-y

THE EUROPEAN PHYSICAL JOURNAL D

Side-on O_2 interaction with heme-based nanomaterials

M. Tsuda, E.S. Dy, and H. Kasai[a]

Department of Precision Science & Technology and Applied Physics, Osaka University, Suita, Osaka 565–0871, Japan

Received 25 July 2005 / Received in final form 16 August 2005

Abstract. We investigate the side-on interaction of O_2 with manganese-porphyrin (MnP) and iron-porphyrin (FeP) using ab initio density functional calculations. The MnP–O_2 adduct takes a side-on configuration in the sextet state while the FeP–O_2 adduct takes it in the singlet state. The O–O bond of the side-on FeP–O_2 is weaker than that of the side-on MnP–O_2 because of more reactive singlet O_2 for the adsorption on the substrate. Moreover, the O_2 dissociation barrier on FeP is lower than that on MnP via the side-on O_2 adduct. It is energetically comparable to that of the well-known platinum catalyst.

PACS. 68.43.Bc Ab initio calculations of adsorbate structure and reactions – 82.20.Kh Potential energy surfaces for chemical reactions – 82.45.Jn Surface structure, reactivity and catalysis

1 Introduction

Metalloporphyrins have received much attention because of their biological significance and unique catalytic properties [1,2] in addition to their spectroscopic, magnetic and electrochemical properties. In particular, iron-porphyrin (FeP) is representative of heme, which is the active site of enzymes such as hemoglobin (Hb), myoglobin (Mb) and cytochrome c oxidase (CcO). Hb and Mb transport O_2 molecules in the vascular systems of animals. On the other hand, CcO activates O_2 molecules with a Cu complex in aerobic metabolism. Taking the affinities of heme and O_2 into account, we have tried to apply the O_2/heme systems to fuel-cell cathode catalysts [3–6], where the oxygen reduction reaction (ORR) occurs. Although O–O bond cleavage of O_2 is unambiguously necessary for the ORR, the details of the full ORR mechanism are complicated and still remain unclear.

In binding O_2 to heme, the Fe–O_2 unit is normally bent and takes the asymmetric end-on O_2 configuration (see Fig. 1) due to the two electrons of O_2 in its π^* antibonding orbital [7,8]. In some special cases, however, the symmetric side-on Fe–O_2 configuration (see Fig. 1) has been experimentally suggested in FeP-based systems. The side-on configuration can be trapped at low temperatures upon photoexcitation of FeTPP–O_2 (TPP: tetraphenylporphyrin) adduct [9]. Moreover, Mb–O_2 adduct at low temperatures shows a sizable nonphotolyzable fraction, which has been suggested to arise from isomerization to the side-on structure [10,11]. In the analogous MnTPP–O_2, only the side-on configuration has been confirmed [12], whereas the side-on CoTPP–O_2 and NiTPP–O_2 configurations have not yet been synthesized. Despite the possibility of the side-on O_2 configurations on MnTPP and FeTPP, the details of the side-on MnTPP–O_2 and FeTPP–O_2 interactions from a molecular level, including their energy-state dependence, have yet to be fully understood.

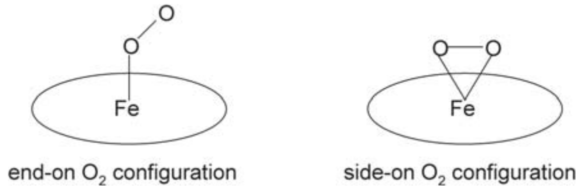

Fig. 1. Schematic representations of end-on and side-on heme-O_2 configurations.

The O–O bond of the side-on O_2 configuration is generally weaker than that of the end-on O_2 configuration because of the greater d–π^* overlap between metal and O_2. This can result in the facile O_2 dissociation. It is also known that the orientation of diatomic molecules affects their dissociative adsorption and associative desorption dynamics on metal surfaces [13,14]. Based on these ideas, we investigate and discuss the side-on O_2 interaction with MnP and FeP in relation to their geometric, vibrational, electronic and energetic properties. Moreover, we consider the catalytic activities of MnP and FeP for O_2 dissociation via their side-on configurations as a first step toward a better understanding of the ORR.

2 Computational details

We perform all calculations based on density functional theory (DFT) [15,16] with the Becke-Perdew-Wang (B3PW91) hybrid exchange-correlation functional [17,18] and the Dunning-Hay-Wadt (LANL2DZ) basis sets [19–22], as implemented in the Gaussian 03 suite

---

[a] e-mail: `kasai@dyn.ap.eng.osaka-u.ac.jp`

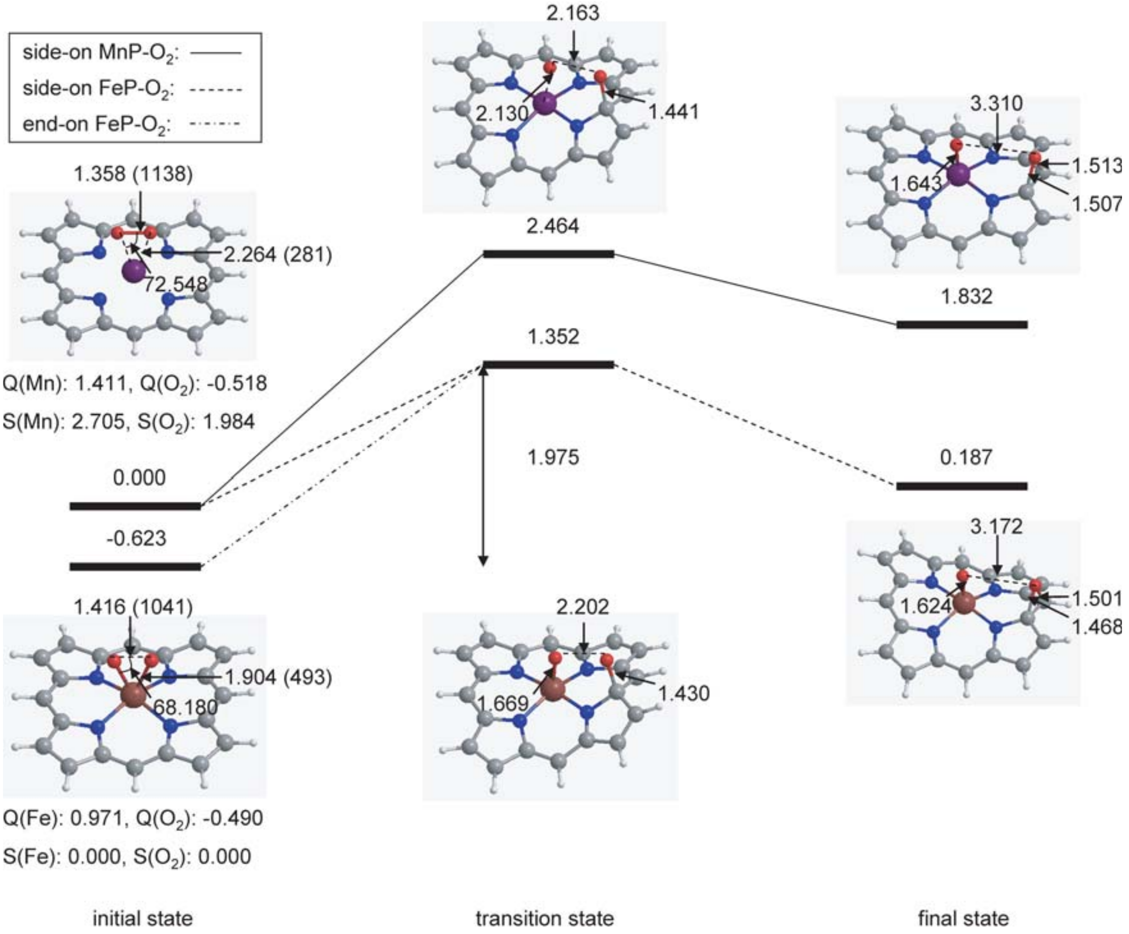

Fig. 2. Calculated potential energy profiles given in eV for O_2 dissociation via the side-on MnP–O_2 and FeP–O_2 adducts. That for O_2 dissociation via the end-on FeP–O_2 is also shown for reference. Distances, angles and stretching frequencies (in parentheses) are given in units of Å, degree and cm^{-1}, respectively. Q and S denote the corresponding atomic/molecular charge and spin population, respectively.

of programs [23]. B3PW91/LANL2DZ level calculations can account for the experimental geometries and vibrational frequencies of metalloporphyrins and their O_2 adducts [3–6]. For the sextet systems, spin contamination can be considered to be negligible because all the calculated $\langle S^2 \rangle$ values vary by less than ~0.3% of the corresponding ideal value of 8.75. All charges and spin populations are presented by the Natural Bond Orbital (NBO) analysis [24]. We searched for possible transition states with the Synchronous Transit-Guided Quasi-Newton (STQN) method [25,26] and confirmed that the transition state we found has only one imaginary frequency.

3 Results and discussion

Figure 2 shows the calculated potential energy profiles for O_2 dissociation via the side-on MnP–O_2 and FeP–O_2 adducts. The reactions initiate from the optimized geometries of the side-on MnP–O_2 and FeP–O_2 adducts, respectively. Our preliminary calculations showed that the MnP–O_2 adduct takes a side-on configuration in the sextet state while the FeP–O_2 adduct takes it in the singlet state. The sextet side-on MnP–O_2 is found to be the ground state as suggested by the infrared (IR) spectroscopy [12]. However, the singlet side-on FeP–O_2 is found to be in the higher energy state than the singlet end-on FeP–O_2. The energy difference between these two FeP–O_2 configurations is 0.623 eV.

In binding O_2 to the substrate, electron transfer occurs from metal to O_2. The elements having smaller electronegativities tend to readily donate their electrons to the antibonding orbitals of O_2. For the side-on MnP–O_2 (FeP–O_2), molecular charge of the O_2 is -0.518 (-0.490). This is consistent with the trend for the electronegativities of Mn and Fe, which are 1.55 and 1.83, respectively. For the side-on MnP–O_2 (FeP–O_2), distance and stretching frequency of the O–O bond are 1.358 Å (1.416 Å) and 1138 cm^{-1} (1041 cm^{-1}). This indicates that the O–O bond of the side-on FeP–O_2 is weaker than that of the MnP–O_2. This is because the singlet O_2, which can be produced by photoexcitation of the triplet O_2, has higher reactivity than the triplet O_2 [27] with respect to the adsorption on the substrate [28–31].

In cleaving the O–O bond, one of the O atoms directly attacks the center of the nearest C–C bond because interaction with the π orbital of the C–C bond is energetically favored. For the side-on MnP–O_2 (FeP–O_2), the O–O distance increases to 2.163 Å (2.202 Å) and the porphyrin ring significantly bends to pick up the separating O atom at the transition state. The O–O bond cleavage requires activation barriers of 2.464 eV (1.352 eV) for the side-on MnP–O_2 (FeP–O_2) [1.975 eV for the end-on FeP–O_2 for reference]. In the side-on MnP–O_2 case, the comparatively weak Mn–O bond formation during the O–O bond cleavage is due to its high-spin state, resulting in the high O_2 dissociation barrier. This is in agreement with the experimental results [32,33] on oxometalloporphyrins that the Mn–O bond is weaker than the Fe–O bond due to the high-spin state of the oxomanganese porphyrin. Here, we compare these activation barriers with those of the well-known platinum catalyst for the purpose of use as a fuel-cell cathode catalyst. Theoretical studies [34,35] from ab initio density functional calculations showed that activation barriers for O_2 dissociative adsorption on Pt(111) vary between ∼0.9 eV and ∼1.7 eV depending on the adsorption sites. Therefore, O_2 dissociation barrier of 1.352 eV via the side-on FeP–O_2 is energetically comparable to those on Pt(111). As a practical application, we suggest that singlet O_2 should be impinged on heme to dissociate O_2 via the side-on orientation.

4 Conclusions

We confirmed the side-on O_2 interaction with MnP and FeP. The singlet side-on FeP–O_2 in the high energy state favors O_2 adsorption and dissociation as compared to the sextet side-on MnP–O_2. Our results suggest that this reaction involving the side-on FeP–O_2, which can compete with the catalytic activity of the well-known Pt, may be realized by impinging singlet O_2.

This work was partly performed under the 21st Century COE program (G18) by Japan Society for the Promotion of Science (JSPS) and "Research and Development of Polymer Electrolyte Fuel Cell Systems" by New Energy and Industrial Technology Development Organization (NEDO). The calculations presented here were carried out using the computer facilities of Japan Atomic Energy Research Institute (JAERI) and Cybermedia Center, Osaka University (CMC).

References

1. D. Dolphin, R.H. Felton, Acc. Chem. Res. **7**, 26 (1974)
2. *The Porphyrins*, edited by D. Dolphin (Academic, New York, 1978)
3. M. Tsuda, W.A. Diño, H. Nakanishi, H. Kasai, e-J. Surf. Sci. Nanotech. **2**, 226 (2004)
4. M. Tsuda, W.A. Diño, H. Nakanishi, H. Kasai, Chem. Phys. Lett. **402**, 71 (2005)
5. M. Tsuda, W.A. Diño, H. Kasai, Jpn J. Appl. Phys. **44**, L57 (2005)
6. M. Tsuda, E.S. Dy, H. Kasai., J. Chem. Phys. **122**, 244719 (2005)
7. C. Rovira, K. Kunc, J. Hutter, P. Ballone, M. Parrinello, J. Phys. Chem. A **101**, 8914 (1997)
8. K.M. Vogel, P.M. Kozlowski, M.Z. Zgierski, T.G. Spiro, J. Am. Chem. Soc. **121**, 9915 (1999)
9. T. Watanabe, T. Ama, K. Nakamoto, J. Phys. Chem. **88**, 440 (1984)
10. M.R. Chance, S.H. Courtney, M.D. Chavez, M.R. Ondrias, J.M. Friedman, Biochemistry **29**, 5537 (1990)
11. L.M. Miller, M. Patel, M.R. Chance, J. Am. Chem. Soc. **118**, 4511(1996)
12. M.W. Urban, K. Nakamoto, F. Basolo, Inorg. Chem. **21**, 3406 (1982)
13. W.A. Diño, H. Kasai, A. Okiji, Prog. Surf. Sci. **63**, 63 (2000)
14. M. Okada, K. Moritani, A. Yoshigoe, Y. Teraoka, H. Nakanishi, W.A. Diño, H. Kasai, T. Kasai, Chem. Phys. **301**, 315 (2004)
15. P. Hohenberg, W. Kohn, Phys. Rev. **136**, B864 (1964)
16. W. Kohn, L.J. Sham, Phys. Rev. **140**, A1133 (1965)
17. A.D. Becke, J. Chem. Phys. **98**, 5648 (1993)
18. J.P. Perdew, Y. Wang, Phys. Rev. B **45**, 13244 (1992)
19. T.H. Dunning Jr, P.J. Hay, in *Modern Theoretical Chemistry*, edited by H.F. Schaefer III (Plenum, New York, 1976), pp. 1–28
20. P.J. Hay, W.R. Wadt, J. Chem. Phys. **82**, 270 (1985)
21. W.R. Wadt, P.J. Hay, J. Chem. Phys. **82**, 284 (1985)
22. P.J. Hay, W.R. Wadt, J. Chem. Phys. **82**, 299 (1985)
23. M.J. Frisch et al., *Gaussian 03*, Revision B.05 (Gaussian, Inc., Pittsburgh PA, 2003)
24. A.E. Reed, L.A. Curtiss, F. Weinhold, Chem. Rev. **88**, 899 (1988)
25. C. Peng, P.Y. Ayala, H.B. Schlegel, M.J. Frisch, J. Comput. Chem. **17**, 49 (1996)
26. C. Peng, H.B. Schlegel, Isr. J. Chem. **33**, 449 (1994)
27. In Figure 2, $S(O_2)$ of 1.984 for the MnP–O_2 indicates that it is almost the triplet O_2
28. Y.F. Zhang, Z.F. Liu, J. Phys. Chem. B **108**, 11435 (2004)
29. Y.J. Xu, J.Q. Li, Chem. Phys. Lett. **400**, 406 (2004)
30. X.L. Fan, Y.F. Zhang, W.M. Lau, Z.F. Liu, Phys. Rev. Lett. **94**, 016101 (2005)
31. J. Behler, B. Delley, S. Lorenz, K. Reuter, M. Scheffler, Phys. Rev. Lett. **94**, 036104 (2005)
32. R.S. Czernuszewicz, Y.O. Su, M.K. Stern, K.A. Macor, D. Kim, J.T. Groves, T.G. Spiro, J. Am. Chem. Soc. **110**, 4158 (1988)
33. R.J. Nick, G.B. Ray, K.M. Fish, T.G. Spiro, J.T. Groves, J. Am. Chem. Soc. **113**, 1838 (1991)
34. A. Eichler, J. Hafner, Phys. Rev. Lett. **79**, 4481 (1997)
35. S. Yotsuhashi, Y. Yamada, W.A. Diño, H. Nakanishi, H. Kasai, Phys. Rev. B **72**, 033415 (2005)